

Computational Model of Energetic Particle Fluxes in the Magnetosphere

Yu Xiang

Thomas Jefferson High School for Science and Technology
Alexandria, VA

January 26, 2006

Contents

Introduction	1
Background	3
Development, Procedures, and Testing	6
Results and Conclusion	16
Appendix	23

Abstract

The Earth's magnetosphere is a region of space dominated by Earth's magnetic fields. Motion of energetic charged particles, such as electrons and protons, in this region is affected mainly by these magnetic fields and the induced electric fields. Computer simulation of particle motion is an important tool for studying energetic particle fluxes in this region because direct observation of their paths proves to be very difficult. Given initial conditions and data on the behavior of magnetic and electric fields, the simulation should be able to calculate and represent the motion of particles in the magnetosphere. This computational model would assist in studying the behavior of charged particles in this region of space.

This project develops software for co-processing energetic particles with the MHD (Magnetohydrodynamics) evolution in a magnetospheric MHD code. This particle-in-cell module would use the data about the magnetic and electric fields calculated from the MHD code to move a number of charged particles, neglecting their own fields, energy depositions, and relativistic effects. In regions where the field conditions satisfy certain constraints, such as the conservation of magnetic moment and small variation in the magnetic field during one gyro period, the fast gyration motion will be neglected, and only the guiding center's movement will be tracked, mostly the north-south bounce, ExB drift, and drift due to magnetic field inhomogeneity. In regions where the approximations of the guiding centers' motions break down, the gyration motion will be calculated at the cost of much higher run time. At each time step, a set of particles would be injected with a spectrum of pitch-angles and energies at various source points on the fixed grid of the MHD code. An interpolation routine will use a matrix of field values calculated from the MHD code to compute the magnetic and electric fields. The position and velocity of these particles will be updated after calculating the effects of the magnetic and electric forces acting upon them, and the new trajectories and energies will be recorded. A simple visualization routine uses these data to give a graphical display of the fields and the particles' paths, which gives a qualitative description of the particles' motions.

Introduction

The goal of this project is to develop software for simulating the motion of energetic particles in the Earth's magnetosphere. Given initial conditions (positions, pitch-angles and energies) of charged particles and data on the behavior of magnetic and electric fields, the computational model will calculate and represent the motion of these particles, including the bounce motion, ExB drift, and drift due to inhomogeneity (transverse gradient and curvature) of the magnetic field. The magnetic and electric fields can be calculated using currently available MHD codes, while the model being developed focuses on calculating the particles' motions using physical laws that relate the movement of charged particles with the configuration of magnetic and electric fields. The particles' own fields, their energy deposition, and relativistic effects are neglected. In regions where the magnetic moment of gyration is nearly invariant, the fast gyration motions of the particles are neglected, and only the motions of the particles' guiding centers are tracked, mostly the north-south bounce and east-west drift. The code will implement mathematical equations describing the particle motion, integrating over discrete time intervals. Approximations are made to lower the complexity of algorithms and reduce runtime. The finished model should be able to calculate the velocities and positions of charged particles at each time step, and record the updated trajectories and energies. These data can be used for further research and analysis. A simple visualization routine is developed in order

to give a graphical display of the fields and the path of the particles. The display can be used to give a qualitative description of the particles' motions and verify the validity of the implementation.

There are limitations to this computational model. The formulas used for calculating the motion of particles' guiding centers and approximations made to reduce complexity and runtime break down at regions of very low magnetic field strength or places where magnetic fields are turbulent and change directions rapidly. The equations describing the motion are integrated over discrete, finite time intervals, limiting the accuracy of the model. The significant amount of computation using floating point numbers might lead to potentially large errors. Also, the amount of computing power available will limit the number of particles that can be simulated simultaneously in order to keep the runtime under a reasonable limit.

Simulations are very important for studying particle fluxes in the magnetosphere because gathering data about particle motion in this region of space is very difficult. The model can provide a great tool for scientists studying the magnetosphere. Another potential application is the prediction of events involving energetic particles in the magnetosphere. Electronic equipment, such as on satellites and orbiting telescopes, can be damaged by collisions with energetic particles. The ability to track the movement of these charged particles can help prevent these accidents and prolong the lifetime of these equipment. Scientists studying the ionosphere, directly underneath the magnetosphere, might find this model useful because disturbances and particle

fluxes in the magnetosphere have direct effects on the ionosphere. This model can also be used as a testing tool for future models of the magnetosphere that improve upon current ones.

Background

Table 1. Some common symbols used

Symbol	Description	Units
\vec{r}	Position	Meters (m)
\vec{V}	Velocity	Meters/Second (m/s)
\vec{F}	Force	Newtons (N)
\vec{E}	Electric Field	Newtons/Coulomb (N/C)
\vec{B}	Magnetic Field	Teslas (T)
m	Mass	Kilograms (kg)
t	Time	Seconds (s)
q	Charge	Coulombs (C)
μ	Magnetic moment	Joules/Tesla (J/T)
α	Pitch angle	Degrees ($^{\circ}$)

Particle motion in the Earth's magnetosphere is dominated by the Earth's magnetic field and the induced electric field as dictated by Maxwell's equations. Near the Earth's surface, the magnetic field is nearly that of a dipole field. As one moves farther into space, the magnetic field gets more complex as the result of interaction with the solar wind, which give the magnetosphere its bullet shape. This project seeks to develop a model that simulates charged particle motion in this region of space and utilizes equations governing the movements of particles in electric and magnetic fields.

Define \vec{V}_{\parallel} and \vec{V}_{\perp} to be the components of the velocity parallel and per-

pendicular, respectively, to the magnetic field. So,

$$\begin{aligned}\vec{V}_{\parallel} &= (\vec{V} \cdot \hat{b})\hat{b} \\ \vec{V}_{\perp} &= \vec{V} - \vec{V}_{\parallel}\end{aligned}$$

where $\hat{b} = \frac{\vec{B}}{B}$.

The magnetic moment, μ , is defined to be,

$$\mu = \frac{mV_{\perp}^2}{2B}$$

This quantity is one of the adiabatic invariants and will be conserved if the magnetic field does not vary by much during one gyration of the particle. If the magnetic moment is well-conserved, the approximations of the guiding center motion will be valid. Otherwise, the program must use a fast time scale and compute the gyro motion at the cost of much longer run time.

The gyro motion of the particle on a fast time scale is described by,

$$\vec{r} = R[\cos(\omega t - \phi)\hat{x} + \sin(\omega t - \phi)\hat{y}]$$

where \vec{r} is with respect to the center of gyration (the guiding center), $R = \frac{mV_{\perp}}{qB}$, $\omega = \frac{qB}{m}$, and the magnetic field is in the \hat{z} direction.

In a combined electric and magnetic field, the change in parallel velocity is given by, $\frac{d\vec{V}_{\parallel}}{dt} = \frac{q}{m} \vec{E}_{\parallel}$ where $\vec{E}_{\parallel} = (\vec{E} \cdot \hat{b})\hat{b}$. On integrating over the fast time scale, the remaining perpendicular motion is broken into two parts,

$$\langle \vec{V}_{\perp} \rangle = \vec{V}_{DB} + \vec{V}_{DE}$$

where \vec{V}_{DB} is the perpendicular drift velocity in a nonuniform static field and \vec{V}_{DE} is given by,

$$\vec{V}_{DE} = \frac{\vec{E} \times \vec{B}}{B^2}$$

\vec{V}_{DE} is the drift motion perpendicular to both the electric and magnetic field. There is another drift motion due to gravitational fields described by $\vec{V}_{DG} = \frac{m}{q} \frac{\vec{g} \times \vec{B}}{B^2}$, which is neglected in the model because its effects are very small compared to the effects of the drift motions due to the crossed electric and magnetic fields and the inhomogeneity of magnetic fields (see appendix for justification).

If a magnetic field has a longitudinal gradient, this variation causes an *effective force* on the *guiding centers* of particles given by,

$$F_{\parallel} = -\mu(\hat{b} \cdot \nabla B)$$

This force is parallel to the magnetic field and causes the north-south bounce motion of the particles.

If the magnetic field has a transverse gradient, there is a drift motion perpendicular to \vec{B} , given by,

$$\vec{V}_{D,grad} = \frac{1}{2} \frac{mV_{\perp}^2}{qB} \frac{\hat{b} \times \nabla B}{B}$$

There is another drift motion similar to $\vec{V}_{D,grad}$ caused by magnetic field curvature,

$$\vec{V}_{DC} = \frac{mV_{\parallel}^2}{qB} \frac{\hat{b} \times \nabla B}{B}$$

Adding $\vec{V}_{D,grad}$ and \vec{V}_{DC} gives the drift motion due to the inhomogeneity of magnetic field \vec{V}_{DB} ,

$$\vec{V}_{DB} = \vec{V}_{D,grad} + \vec{V}_{DC} = \frac{m(V_{\perp}^2 + 2V_{\parallel}^2)}{2qB^2} (\hat{b} \times \nabla B)$$

The drift motion due to the crossed electric and magnetic fields and inhomogeneity of \vec{B} give rise to the slow east-west drift of particles in the magnetosphere. The north-south bounce motion is the result of the conservation of magnetic moment and energy in the absence of an electric field. As a particle moves to a region of greater magnetic field strength, V_{\perp} must increase in order to conserve $\frac{mV_{\perp}}{2B}$, which would cause a decrease in V_{\parallel} in order for the energy ($\frac{1}{2}mV_{\perp}^2 + \frac{1}{2}mV_{\parallel}^2$) to be conserved. The points at which V_{\parallel} is 0 are known as mirror points; the particle bounces back and forth between two mirror points. In the presence of electric fields, the particles continue to undergo bounce and drift motion but the paths will be irregular due to variations in energies and magnetic moments caused by work done by the electric field.

This project will combine these equations describing particle motion to create a model that calculates and follows the movement of charged particles in the magnetosphere.

Development, Procedures, and Testing

This model involves implementing mathematical equations and doing vector calculations, so Fortran 90 is chosen to code the computational part of this project. Developed for numerical calculations, Fortran 90 is the ideal language to use. Mathematical equations are easily implemented in Fortran

90 since the language originated in order to translate formulas to computer programs. One disadvantage of Fortran 90 is that it offers very little graphics capabilities; so, C++ was chosen for the development of the visualization routine. OpenGL, a set of graphical libraries available in C++, is used for visualization because of its versatility and portability. The standard OpenGL libraries and the open-source GLUT (OpenGL Utility Toolkit) are the main tools for developing the visualization routine; they give the programmer full control over how objects are displayed on the screen.

Physical constants are programmed into a separate module called Constants. Any other part of the code that utilizes these constants can simply import the Constants module. To keep the units consistent, the international standard system of units (SI) is used.

Table 2. Constants

Constant name	Description	Value
Pi	π	3.14159265358979
LightSpeed	c	3.0e8 m/s
Eps	A small value to distinguish floating point numbers	2e-31
ElectronCharge	Unit charge	1.60217646e-19 C
ProtonMass	Mass of a proton	1.67262158e-27 kg
ElectronMass	Mass of an electron	9.10938188e-31 kg
EarthRadius	Radius of Earth (R_e)	6.3781e6 m
Bo	Magnetic field strength at the Earth's surface	0.35e-4 T

The coordinate system chosen for this project is the ordinary cartesian coordinate system: \hat{z} is in the northward direction of the Earth's magnetic dipole axis, \hat{x} points from the center of Earth toward the Sun, and \hat{y} is such

that $\hat{x} \times \hat{y} = \hat{z}$. However, calculations are often easier if polar coordinates are used, so the conversion from cartesian to polar coordinates and vice versa are programmed in the Functions module. One important language-specific problem was that the atan2 function in Fortran 90 only returns values that are in the 1st and 4th quadrant, appropriate adjustments to ϕ must be made if the points are positioned in the 2nd and 3rd quadrant.

Because the electric and magnetic field will be calculated using available MHD code with discrete grid points, the fields must be interpolated since the particles' positions will not necessarily coincide with the grid points. The simple Lagrange polynomial interpolation is used. Given three points (x_1, y_1) , (x_2, y_2) , and (x_3, y_3) , the interpolation function $P(x)$ is,

$$P(x) = \frac{(x - x_2)(x - x_3)}{(x_1 - x_2)(x_1 - x_3)}y_1 + \frac{(x - x_1)(x - x_3)}{(x_2 - x_1)(x_2 - x_3)}y_2 + \frac{(x - x_1)(x - x_2)}{(x_3 - x_1)(x_3 - x_2)}y_3$$

To generalize this interpolation to the three spatial dimensions and time, the program calculates four polynomials with three being the interpolation over space and one being the interpolation over time.

Gradient of the magnetic field is necessary for calculations, but is not given by the MHD code. The model uses the components of the magnetic field in the neighboring points to calculate the gradient at any particular grid point. Suppose the $n \times n \times n$ matrix contains the values for the components of the magnetic field at the n^3 number of grid points with grid sizes of dimension $\Delta x \times \Delta y \times \Delta z$ and the actual position of the grid point (i, j, k) is

$(x_{min} + (i - 1)\Delta x, y_{min} + (j - 1)\Delta y, z_{min} + (k - 1)\Delta z)$ where $(x_{min}, y_{min}, z_{min})$ is the position of grid point $(1, 1, 1)$, the gradient of the magnetic field at grid point (i, j, k) for $1 < i < n, 1 < j < n, 1 < k < n$ is calculated by using the following scheme,

Define $\text{Max}(a,b)=a$ if $|a| > |b|$, b other wise,

$$\begin{aligned} \nabla B(i, j, k) = & \text{Max}\left(\frac{B_x(i + 1, j, k) - B_x(i, j, k)}{\Delta x}, \frac{B_x(i, j, k) - B_x(i - 1, j, k)}{\Delta x}\right)\hat{x} + \\ & \text{Max}\left(\frac{B_y(i, j + 1, k) - B_y(i, j, k)}{\Delta y}, \frac{B_y(i, j, k) - B_y(i, j - 1, k)}{\Delta y}\right)\hat{y} + \\ & \text{Max}\left(\frac{B_z(i, j, k + 1) - B_z(i, j, k)}{\Delta z}, \frac{B_z(i, j, k) - B_z(i, j, k - 1)}{\Delta z}\right)\hat{z} \end{aligned}$$

These values for the gradient of the magnetic field are stored in a separate matrix. The same interpolation technique used for calculating the magnetic field is used to interpolate the field gradient at the desired spatial point.

Vector calculations are crucial to this project; an entire module (appropriately named Vectors) is devoted to vector functions. A custom data structure called Vector is made to store the cartesian coordinates of the vectors. Commonly used vector operations are coded in this module with all calculations done using cartesian coordinates.

$$\begin{aligned} \left|\vec{A}\right| &= A = \sqrt{A_x^2 + A_y^2 + A_z^2} \\ \hat{A} &= \frac{\vec{A}}{A} \\ \vec{A} + \vec{B} &= (A_x + B_x)\hat{i} + (A_y + B_y)\hat{j} + (A_z + B_z)\hat{k} \\ \vec{A} \cdot \vec{B} &= A_x B_x + A_y B_y + A_z B_z \end{aligned}$$

$$\vec{A} \times \vec{B} = (A_y B_z - B_y A_z) \hat{i} + (B_x A_z - A_x B_z) \hat{j} + (A_x B_y - A_y B_x) \hat{k}$$

Data structures representing the particles are programmed to store the necessary information during the simulation. The model must keep track of a particle's mass, charge, position, parallel velocity, perpendicular velocity, drift velocity, energy, and magnetic moment.

An initialization routine that takes the particle's mass, charge, position, pitch-angle (angle between velocity vector and magnetic field vector), energy(in eV), and electric and magnetic fields at the initial position calculates the rest of the data about this particle: parallel velocity, perpendicular velocity, drift, and magnetic moment. The algorithm first converts the pitch-angle (α) to radians and the energy from units of electron volts to joules. The rest of the calculations are as follows,

$$V = \sqrt{\frac{2 * \text{Energy}}{\text{mass}}}$$

$$V_{\perp} = V \sin(\alpha), V_{\parallel} = V \cos(\alpha)$$

$$\mu = \frac{m V_{\perp}^2}{2B}$$

$$\vec{V}_{drift} = \frac{\vec{E} \times \vec{B}}{B^2} + \frac{m(V_{\perp}^2 + 2V_{\parallel}^2)}{2qB^2} (\hat{b} \times \nabla B)$$

At each time step, a separate routine adjusts the time interval appropriately to ensure the code runs as fast as possible while retaining a certain degree of accuracy. The magnetic field is first checked to see if they satisfy the following condition,

$$R \frac{|\nabla B|}{|B|} \ll 1$$

where R is the radius of gyration given by,

$$R = \frac{mV_{\perp}}{qB}$$

If the magnetic field satisfy this condition, the magnetic moment will be well-conserved, so the approximations of the guiding center motions are valid and a slow time scale will be used. Otherwise, the fast gyro motion cannot be neglected so the program goes into a fast time scale and calculates the circular motion of the particle.

The two parts of the drift velocity are obtained from two separate routines that calculate the ExB drift and the magnetic field inhomogeneity drift. The implementation of the ExB drift is fairly straight forward: take the cross product of electric and magnetic field, then divide the result by the square of the magnetic field strength. To avoid unnecessary floating point operations, a variable is used to store the value $\frac{1}{B^2}$ and B^2 is calculated by summation of the square of the components of the magnetic field. To keep calculations as precise as possible, this technique of using temporary variables and summation of the square of the components is used throughout the programming of this model. The magnetic field inhomogeneity drift is implemented in a similar manner, using variables to temporarily store values and manipulating them to give the desired result.

The positions and velocities of the particle are updated in the Move subroutine. The drift motion is first updated, then the force exerted on the parti-

cle by the electric field and the effective longitudinal force ($F_{\parallel} = -\mu(\hat{b} \cdot \nabla B)$) are used to calculate the acceleration. The position change is obtained by combining the updated drift motion and the acceleration. The last step is to update parallel velocity, perpendicular velocity, position, and energy by adding the respective changes.

If the fast gyro motion cannot be neglected because the magnetic moment is not well conserved, the time intervals must be reduced and the particles' trajectories will be updated using the Lorentz force law,

$$m \frac{d^2 \vec{r}}{dt^2} = q \vec{E} + q \vec{V} \times \vec{B}$$

The frequency (ω) and radius (R) of gyration is given by,

$$\omega = \left| \frac{qB}{m} \right|, R = \left| \frac{mV_{\perp}}{qB} \right|$$

Let $\hat{e} = \frac{\vec{V}_{\perp}}{V_{\perp}}$, then $\hat{e} \times \hat{b}$ is parallel to the vector pointing from the center of gyration to the particle's position. Let \vec{r} be the position of the particle with respect to the gyro center and take time t to be 0 as the beginning of the current time step, then,

for $q < 0$,

$$\begin{aligned} \vec{r}_0 &= R(\hat{e} \times \hat{b}) \\ \vec{r} &= R [\sin(\omega t)\hat{e} + \cos(\omega t)\hat{e} \times \hat{b}] \\ \vec{V}_{\perp} &= \frac{d\vec{r}}{dt} = \omega R [\cos(\omega t)\hat{e} - \sin(\omega t)\hat{e} \times \hat{b}] \end{aligned}$$

for $q > 0$,

$$\begin{aligned}\vec{r}_0 &= -R(\hat{e} \times \hat{b}) \\ \vec{r} &= R [\sin(\omega t)\hat{e} - \cos(\omega t)\hat{e} \times \hat{b}] \\ \vec{V}_\perp &= \frac{d\vec{r}}{dt} = \omega R [\cos(\omega t)\hat{e} + \sin(\omega t)\hat{e} \times \hat{b}]\end{aligned}$$

The effect of the electric field is an acceleration of the particle parallel to the field. The particle's position, its guiding center's position, and energy are updated after finishing the calculations for the effects of the magnetic and electric forces acting on the particle.

The main program (named Main) is coded as the central driver that controls the whole simulation. The primary purpose of this module is to read input, make the appropriate calls to functions and subroutines for calculations, and write the output to data files. The visualization routine written in C++ reads the data files, makes appropriate scaling to the numbers for proper display, and creates a graphics representing the data for easy viewing. Keyboard control is programmed into this visualization routine so that the paths of the particles and the fields can be viewed from different angles.

For testing, the Earth's magnetic field is simulated as a static dipole field described by,

$$\begin{aligned}\vec{B} &= B_0 \frac{Re^3}{r^3} [\sin(\theta)\hat{i}_\lambda - 2\cos(\theta)\hat{i}_r] \\ \nabla B &= B_0 \frac{Re^3}{r^3} [\sqrt{(1+3\sin^2(\lambda))}(\frac{-3}{r})\hat{i}_r + \frac{(\frac{3}{r})\sin(\lambda)\cos(\lambda)}{\sqrt{(1+3\sin^2(\lambda))}}\hat{i}_\lambda]\end{aligned}$$

where B_0 is the magnetic field strength at the Earth's surface, about 0.35e-4 T, r is the distance from the Earth's center, θ is the angle the position vector makes with \hat{z} , and $\lambda = \frac{\pi}{2} - \theta$. Converting to cartesian coordinates

and separating into the three components yields,

$$B_x = B_0 \frac{Re^3}{r^3} [-3 \sin(\theta) \cos(\theta) \cos(\phi)]$$

$$B_y = B_0 \frac{Re^3}{r^3} [-3 \sin(\theta) \cos(\theta) \sin(\phi)]$$

$$B_z = B_0 \frac{Re^3}{r^3} [\sin^2(\theta) - 2 \cos^2(\theta)]$$

$$\text{Define } \epsilon = \frac{3}{r} \sqrt{(1 + 3 \sin^2(\lambda))}, \delta = \frac{(\frac{3}{r}) \sin(\lambda) \cos(\lambda)}{\sqrt{(1 + 3 \sin^2(\lambda))}}$$

$$(\nabla B)_x = B_0 \frac{Re^3}{r^3} [-\epsilon \sin(\theta) \cos(\phi) - \delta \cos(\theta) \cos(\phi)]$$

$$(\nabla B)_y = B_0 \frac{Re^3}{r^3} [-\epsilon \sin(\theta) \sin(\phi) - \delta \cos(\theta) \sin(\phi)]$$

$$(\nabla B)_z = B_0 \frac{Re^3}{r^3} [-\epsilon \cos(\theta) + \delta \sin(\theta)]$$

The bounce period of a particle in the described field is given by,

$$T_B \approx 4 \frac{R_0}{V_0} [1.3 - 0.56 \sin \alpha_0]$$

where R_0 is the initial distance from the Earth center, and V_0 is the velocity of the particle when it's at the magnetic equator during its bounce motion.

The magnetic field strength at the mirror points is,

$$B_{tp} = B_0 (1 + \cot^2 \alpha_0)$$

where B_0 is the field strength at the magnetic equator.

The drift period of a particle is,

$$T_D \approx \frac{2\pi R_0^2 q B_0}{3V_0^2 m} [0.35 + 0.15 \sin^2 \alpha_0]^{-1}$$

The electric field arising from the motion of the ionosphere through the dipole field is described by,

$$\vec{E}_c = -\frac{\omega B_0 R_e^3}{r^2} \cos(\lambda) [2 \sin(\lambda) \hat{i}_\lambda + \cos(\lambda) \hat{i}_r]$$

where ω is the angular frequency of the Earth's rotation.

Another source of electric field is the motion of the solar wind,

$$\vec{E}_{sw} = \frac{\omega B_0 R_e^3}{r^2} \hat{y}$$

Adding \vec{E}_c and \vec{E}_{sw} yields the total electric field,

$$\text{Define } E_0 = \frac{\omega B_0 R_e^3}{r^2}$$

$$\vec{E} = \vec{E}_c + \vec{E}_{sw} = E_0 [\hat{y} - 2 \sin \lambda \cos \lambda \hat{i}_\lambda - \cos^2 \lambda \hat{i}_r]$$

Converting to cartesian coordinates,

$$E_x = E_0 [2 \sin \lambda \cos \lambda \cos \theta \cos \phi - \cos^2 \lambda \sin \theta \cos \phi]$$

$$E_y = E_0 [1 + 2 \sin \lambda \cos \lambda \cos \theta \sin \phi - \cos^2 \lambda \sin \theta \sin \phi]$$

$$E_z = E_0 [-2 \sin \lambda \cos \lambda \sin \theta - \cos^2 \lambda \cos \theta]$$

Using the developed model to follow a particle in the static dipole field (without the electric field) and comparing the bounce time, drift period, and magnetic field strength with the expected values will give a measure of the validity of the algorithms and implementations. Adding in the effects of the electric field should yield a fluctuating energy of the particle and slight changes in the particle's trajectory (this change would become less significant for particles with higher energies).

Results and Conclusion

Testing shows that the model simulates particle motion correctly. The interpolated fields closely match the field calculated directly from the formula. The expected north-south bounce motion is evidenced by the parallel arcs formed by the path of the guiding center. The slow east-west drift motion is also observed because the arcs do not overlap completely. The guiding center's path does have the expected symmetry about its midpoint (the magnetic equator, which lies on the xy -plane). The observed values of bounce time, drift period, and mirror point field strength closely match those expected from analytical calculations.

The code is modularized into several components, with each component doing a specific subset of the calculations. Division of the code into modules simplifies the debugging process and makes the code easy to read. The overall structure of the program developed for this model can be summarized by the following diagram.

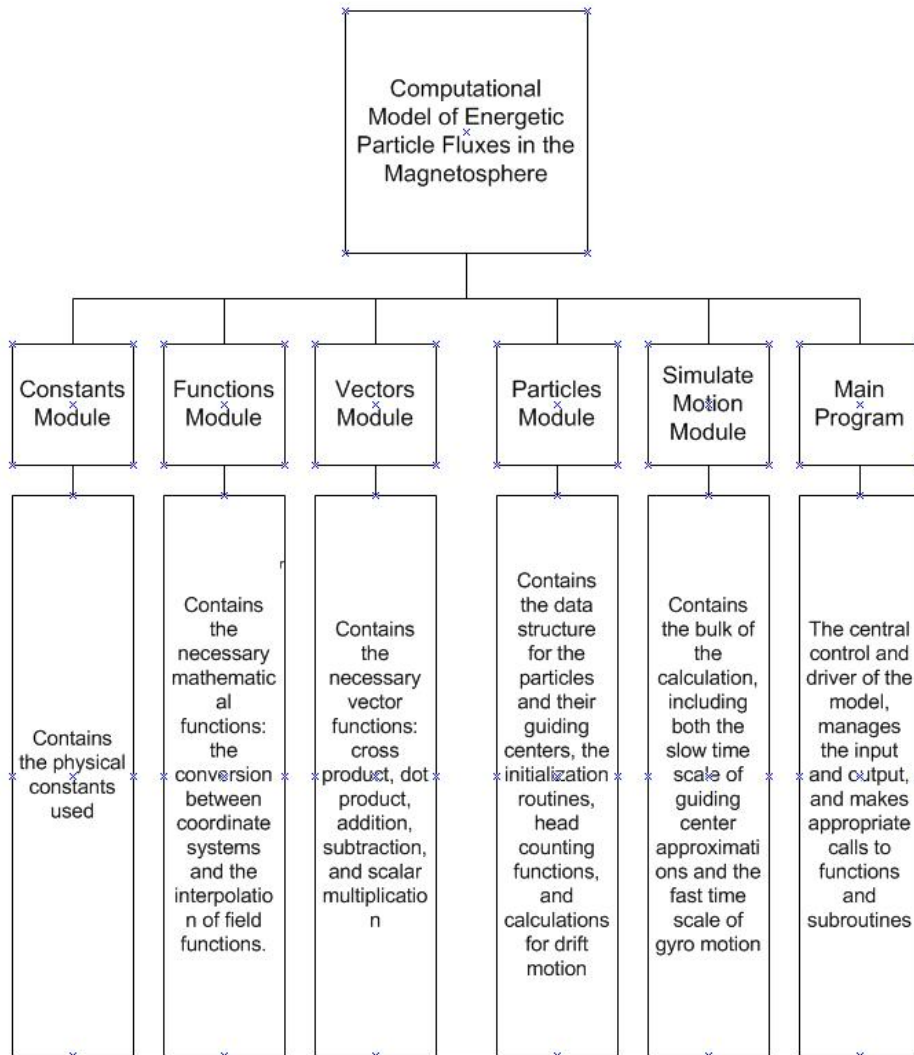


Figure 1. Structure of the Computational Model

Shown in figure 2 is the magnetic field calculated directly from the formula with the window range of $[-20R_e, 20R_e]$ in all three directions.

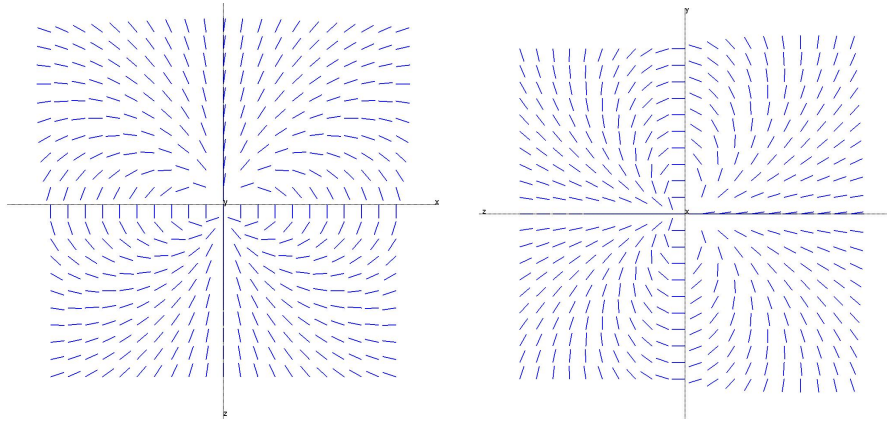


Figure 2. Magnetic Field from the Formula

Shown in figure 3 is the interpolated field from a table containing the values for the magnetic field at discrete grid points with grid sizes of 0.4 Earth radii in each direction.

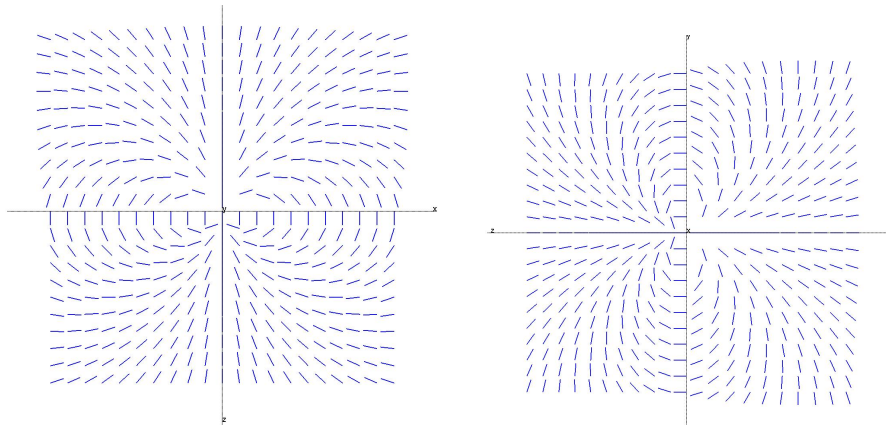


Figure 3. Interpolated Magnetic Field

Shown in figure 4 is the electric field calculated directly from the formula with the window range of $[-20R_e, 20R_e]$ in all three directions.

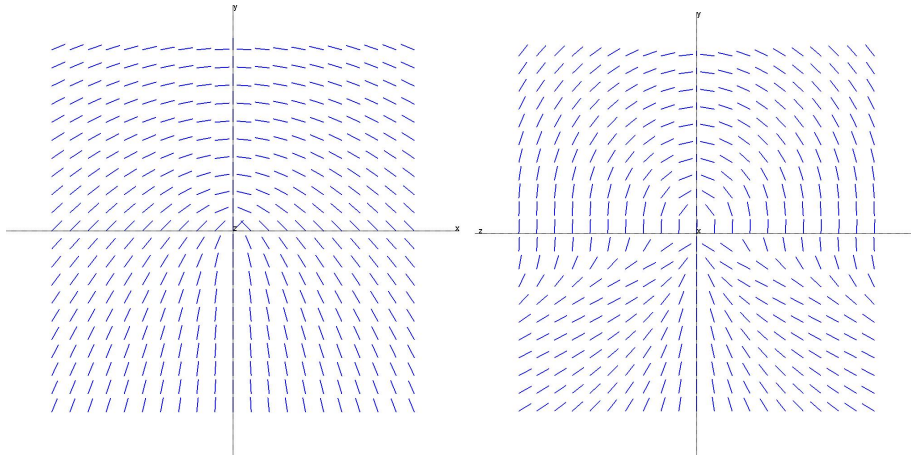


Figure 4. Electric Field from the Formula

Shown in figure 5 is the interpolated field from a table containing the values for the electric field at discrete grid points with grid sizes of 0.4 Earth radii in each direction.

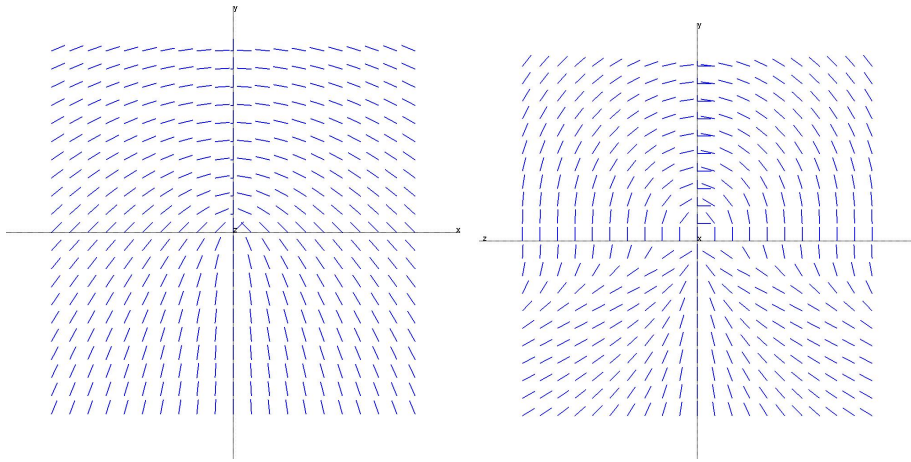


Figure 5. Interpolated Electric Field

Figure 6 shows the calculated path for a 1 KeV proton with an initial pitch-angle of 60° and initial position of $(0, 5R_e, 0)$, tracked for 2 hours.

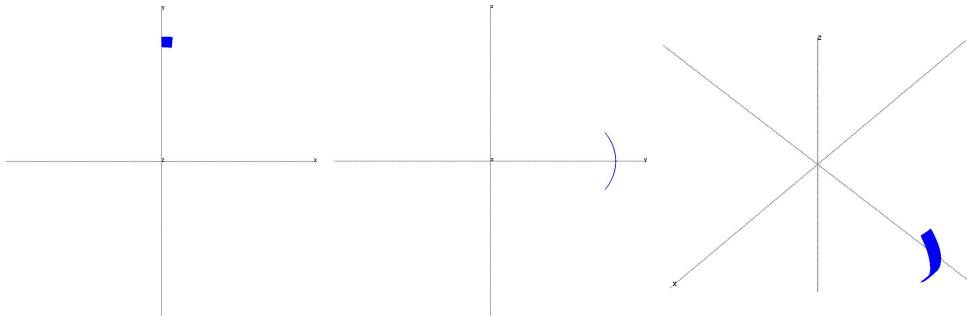


Figure 6. Path of Guiding Center for 1 KeV Proton

Shown in figure 7 is the calculated path of a 10 KeV proton with an initial pitch-angle of 30° and initial position of $(0, 10R_e, 0)$, tracked for 3 hours, slightly longer than a quarter of the expected drift period.

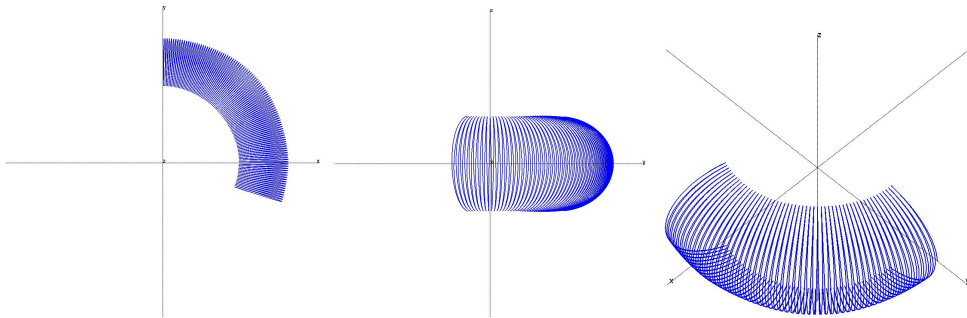


Figure 7. Path of Guiding Center for 10 KeV Proton

Figure 8 shows the path of a 100 KeV proton with an initial pitch-angle of 45° and initial position of $(0, 15R_e, 0)$, tracked for 40 minutes, slightly longer than one drift period.

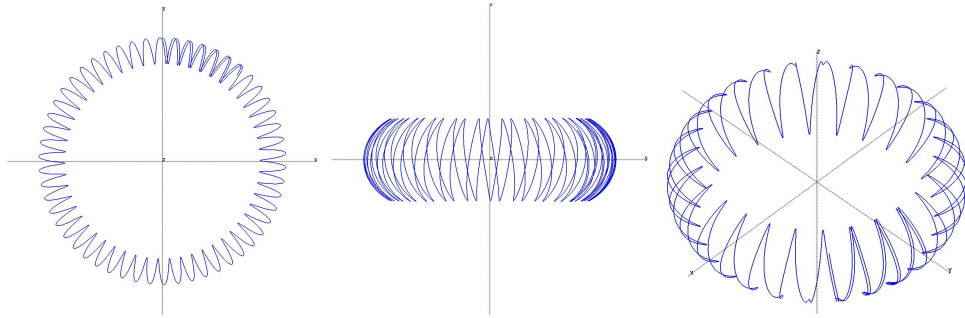


Figure 8. Path of Guiding Center for 100 KeV Proton

Shown in figure 9 is the trajectory of these three particles in the combined electric and magnetic field. As expected, there is a significant change in the path of the 1 KeV proton, a smaller change in the path of the 10 KeV proton, and almost no perceivable change in the trajectory of the 100 KeV proton.

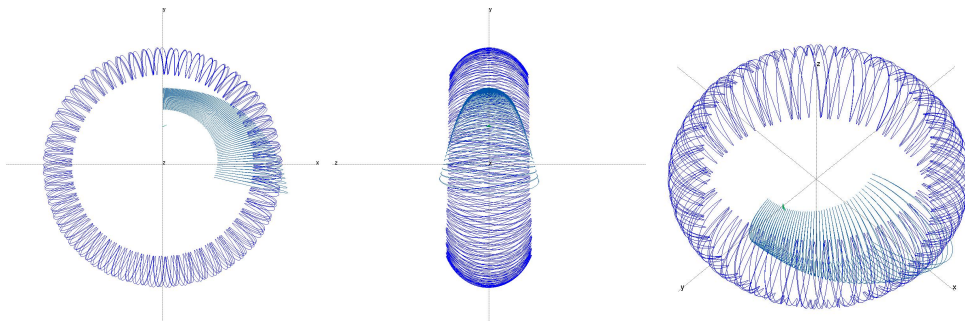


Figure 9. Path of Guiding Center for all three particles

In all three sample runs, the particle's guiding center path exhibits the expected symmetry about the xy -plane. The particle completes the expected proportion of its orbit around the origin during the length of the simulation. For more details, test data for the three trial runs are shown in the appendix.

Figure 10 shows the trajectories of three 1 MeV protons with initial pitch-angle of 45° and initial positions of $(0, 6R_e, 0)$, $(0, 10R_e, 0)$, and $(0, 14R_e, 0)$, tracked for 10 minutes.

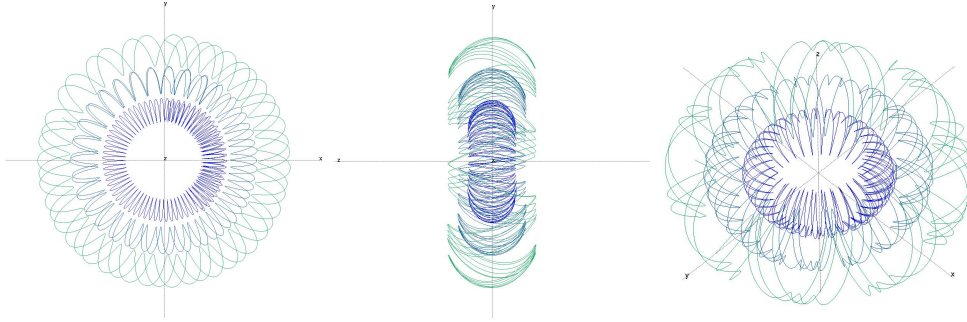


Figure 10. Path of Guiding Center for three 1 MeV Protons

Because of their relatively high energy, the trajectory change due to the electric field is barely observable. Shown in the appendix is the test data for this sample run, where the effects of the electric field is evidenced by the fluctuating energies of the particles.

The project is successful in creating a computational model for energetic particle motion in the Earth's magnetosphere. Further optimization and correction to the code can be done to improve precision and accuracy. Parallelizing and running the code on parallel machines can greatly improve performance. Combined with available magnetohydrodynamics codes, this program can give a complete model that includes both particle motion and field behaviors in the magnetosphere.

Appendix

Here, a simple justification for neglecting the gravitational drift is shown.

The gravitational drift is given by,

$$\vec{V}_{DG} = \frac{m}{q} \frac{\vec{g} \times \vec{B}}{B^2}$$

In a dipole magnetic field, the drift due to the field inhomogeneity is given by,

$$\vec{V}_{DB} = \frac{m}{2qB} (V_{\perp}^2 + 2V_{\parallel}^2) \frac{3}{r} \frac{[1 + \sin^2(\lambda)]}{[1 + 3\sin^2(\lambda)]^{\frac{3}{2}}} \cos(\lambda) \hat{i}_{\phi}$$

The ratio of the magnitude of the gravitational drift and the magnitude of the inhomogeneity drift, approximately $\frac{gR_e}{V^2}$, is very small for typical energetic particles in the magnetosphere because these particles have speeds much greater than $\sqrt{gR_e} \approx 8000 \text{ m/s}$. For example, a 10 KeV proton has speed of about $1.36 \times 10^6 \text{ m/s}$, the ratio $\frac{gR_e}{V^2}$ is approximately 3.34×10^{-5} . Since this ratio is small enough ($\ll 1$) to be neglected, the gravitational drift can be safely neglected.

Shown below is the data for the three trial runs with 0 electric field. Please note that the bounce period is the time it takes for the particle to complete the entire orbit, so the time between two successive bounces is actually half of the bounce time. As seen from the data, the observed values from the simulation closely match the expected ones.

Trial run #1:

Mass: 1.6726215800000000E-027 Charge: 1.6021764600000000E-019

Energy: 1000.000000000000 Pitch Angle: 60.00000000000000
 Initial Position: 0.00000000000000 5.00000000000000 0.00000000000000
 Bo: 2.793441558757901E-007 Vo: 437694.736843198
 Bounce Time: 237.531552539925 Btp: 3.724588619681692E-007
 Average drift period: 619921.466241138

Bounce:Time:	54.9813999941543	Magnetic Field Strength:	3.568702105257149E-007
Bounce:Time:	165.398597204781	Magnetic Field Strength:	3.568416882215171E-007
Bounce:Time:	275.830194415044	Magnetic Field Strength:	3.568849204341854E-007
Bounce:Time:	386.271391625065	Magnetic Field Strength:	3.568523331315427E-007
Bounce:Time:	496.693188835576	Magnetic Field Strength:	3.569007347347626E-007
Bounce:Time:	607.130986045682	Magnetic Field Strength:	3.568631270875101E-007
Bounce:Time:	717.575183255627	Magnetic Field Strength:	3.569178148853423E-007
Bounce:Time:	828.044980464925	Magnetic Field Strength:	3.568750953781652E-007
Bounce:Time:	938.546577673420	Magnetic Field Strength:	3.569365690812451E-007
Bounce:Time:	1049.03877488215	Magnetic Field Strength:	3.568879941809303E-007
Bounce:Time:	1159.58877208942	Magnetic Field Strength:	3.569563207405882E-007
Bounce:Time:	1270.13516929679	Magnetic Field Strength:	3.569024853942771E-007
Bounce:Time:	1380.66936650446	Magnetic Field Strength:	3.569779733682446E-007
Bounce:Time:	1491.20936371198	Magnetic Field Strength:	3.569186955023080E-007
Bounce:Time:	1601.78796091853	Magnetic Field Strength:	3.570011445200711E-007
Bounce:Time:	1712.40835812403	Magnetic Field Strength:	3.569367268653169E-007
Bounce:Time:	1823.04155532920	Magnetic Field Strength:	3.570262176775409E-007
Bounce:Time:	1933.67755253430	Magnetic Field Strength:	3.569567313458448E-007
Bounce:Time:	2044.33954973874	Magnetic Field Strength:	3.570528125816698E-007
Bounce:Time:	2155.01594694282	Magnetic Field Strength:	3.569789683947163E-007
Bounce:Time:	2265.69514414683	Magnetic Field Strength:	3.570813734510911E-007
Bounce:Time:	2376.38874135047	Magnetic Field Strength:	3.570034595828976E-007
Bounce:Time:	2487.09513855379	Magnetic Field Strength:	3.571118005982186E-007
Bounce:Time:	2597.81433575679	Magnetic Field Strength:	3.570304796602809E-007
Bounce:Time:	2708.53373295978	Magnetic Field Strength:	3.571442571920772E-007
Bounce:Time:	2819.28173016205	Magnetic Field Strength:	3.570599801894743E-007
Bounce:Time:	2930.04252736400	Magnetic Field Strength:	3.571789152132108E-007
Bounce:Time:	3040.80672456586	Magnetic Field Strength:	3.570921776453650E-007
Bounce:Time:	3151.59632176708	Magnetic Field Strength:	3.572154710903216E-007
Bounce:Time:	3262.38611896829	Magnetic Field Strength:	3.571271375836540E-007
Bounce:Time:	3373.18871616918	Magnetic Field Strength:	3.572542716245198E-007
Bounce:Time:	3484.01831336939	Magnetic Field Strength:	3.571919746960636E-007
Bounce:Time:	3594.84491056968	Magnetic Field Strength:	3.572797000543227E-007
Bounce:Time:	3705.69930776926	Magnetic Field Strength:	3.572010890441551E-007
Bounce:Time:	3816.54590496904	Magnetic Field Strength:	3.572846276218874E-007
Bounce:Time:	3927.41890216815	Magnetic Field Strength:	3.572683925885267E-007
Bounce:Time:	4038.29829936710	Magnetic Field Strength:	3.573502795382945E-007
Bounce:Time:	4149.19209656569	Magnetic Field Strength:	3.573386216790086E-007
Bounce:Time:	4260.08909376420	Magnetic Field Strength:	3.574185821691229E-007
Bounce:Time:	4370.98769096266	Magnetic Field Strength:	3.574115784742683E-007
Bounce:Time:	4481.90228816072	Magnetic Field Strength:	3.574888947300018E-007
Bounce:Time:	4592.82968535846	Magnetic Field Strength:	3.574873785877151E-007
Bounce:Time:	4703.76668255596	Magnetic Field Strength:	3.575614750070541E-007
Bounce:Time:	4814.71647975313	Magnetic Field Strength:	3.575657086568309E-007
Bounce:Time:	4925.67427695010	Magnetic Field Strength:	3.576362578801283E-007
Bounce:Time:	5036.58427414828	Magnetic Field Strength:	3.576466483273033E-007
Bounce:Time:	5147.57887134432	Magnetic Field Strength:	3.577129067482529E-007
Bounce:Time:	5258.50966854197	Magnetic Field Strength:	3.577294318112126E-007
Bounce:Time:	5369.51066573785	Magnetic Field Strength:	3.577908926427756E-007
Bounce:Time:	5480.53886293304	Magnetic Field Strength:	3.578145099389330E-007
Bounce:Time:	5591.52706012924	Magnetic Field Strength:	3.578703136804444E-007
Bounce:Time:	5702.51365732549	Magnetic Field Strength:	3.579013783967972E-007

Bounce:Time:	5813.56585452007	Magnetic Field Strength:	3.579512235590205E-007
Bounce:Time:	5924.62445171450	Magnetic Field Strength:	3.579904651580603E-007
Bounce:Time:	6035.64464890989	Magnetic Field Strength:	3.580335541613258E-007
Bounce:Time:	6146.72564610375	Magnetic Field Strength:	3.580815472731392E-007
Bounce:Time:	6257.76824329857	Magnetic Field Strength:	3.581164418882529E-007
Bounce:Time:	6368.81424049332	Magnetic Field Strength:	3.581739567469777E-007
Bounce:Time:	6479.86663768790	Magnetic Field Strength:	3.581992701936011E-007
Bounce:Time:	6590.93183488215	Magnetic Field Strength:	3.582706134983095E-007
Bounce:Time:	6702.00343207625	Magnetic Field Strength:	3.582829518841025E-007
Bounce:Time:	6813.07462927036	Magnetic Field Strength:	3.583637956920008E-007
Bounce:Time:	6924.22942646235	Magnetic Field Strength:	3.583703038513755E-007
Bounce:Time:	7035.33462365560	Magnetic Field Strength:	3.584577030358655E-007
Bounce:Time:	7146.44902084861	Magnetic Field Strength:	3.584586819018179E-007

Trial run #2:

Mass: 1.672621580000000E-027 Charge: 1.602176460000000E-019
Energy: 10000.000000000 Pitch Angle: 30.0000000000000
Initial Position: 0.000000000000000 10.0000000000000 0.000000000000000
Bo: 3.500000093481503E-008 Vo: 1384112.28829252
Bounce Time: 188.009649165710 Btp: 1.399999966729610E-007
Average drift period: 35082.4894327844

Bounce:Time:	44.6733562496665	Magnetic Field Strength:	1.238300692311603E-007
Bounce:Time:	134.507753980259	Magnetic Field Strength:	1.237699772294622E-007
Bounce:Time:	224.328951711184	Magnetic Field Strength:	1.238220242805301E-007
Bounce:Time:	314.100749443358	Magnetic Field Strength:	1.239053167074451E-007
Bounce:Time:	403.809347177128	Magnetic Field Strength:	1.240212944074672E-007
Bounce:Time:	493.491344911570	Magnetic Field Strength:	1.242719890208623E-007
Bounce:Time:	583.170942646073	Magnetic Field Strength:	1.243829186928200E-007
Bounce:Time:	672.851140380561	Magnetic Field Strength:	1.245194372385673E-007
Bounce:Time:	762.543138114750	Magnetic Field Strength:	1.246591834777028E-007
Bounce:Time:	852.267135848131	Magnetic Field Strength:	1.247740584946304E-007
Bounce:Time:	942.023933580684	Magnetic Field Strength:	1.249203508210834E-007
Bounce:Time:	1031.82833131203	Magnetic Field Strength:	1.250764465391599E-007
Bounce:Time:	1121.70072904167	Magnetic Field Strength:	1.251391014285014E-007
Bounce:Time:	1211.65092676933	Magnetic Field Strength:	1.252597557341936E-007
Bounce:Time:	1301.68992449476	Magnetic Field Strength:	1.254234783561886E-007
Bounce:Time:	1391.82692221770	Magnetic Field Strength:	1.255960922883689E-007
Bounce:Time:	1482.07251993791	Magnetic Field Strength:	1.257680650805119E-007
Bounce:Time:	1572.44371765494	Magnetic Field Strength:	1.258919449589782E-007
Bounce:Time:	1662.96131536827	Magnetic Field Strength:	1.260708366573572E-007
Bounce:Time:	1753.62991307779	Magnetic Field Strength:	1.262164438969581E-007
Bounce:Time:	1844.46031078322	Magnetic Field Strength:	1.264055150433070E-007
Bounce:Time:	1935.47610848397	Magnetic Field Strength:	1.265410604753954E-007
Bounce:Time:	2026.67390618012	Magnetic Field Strength:	1.267380382470115E-007
Bounce:Time:	2118.07110387123	Magnetic Field Strength:	1.269448674137854E-007
Bounce:Time:	2209.68390155690	Magnetic Field Strength:	1.271531767152255E-007
Bounce:Time:	2301.51669923701	Magnetic Field Strength:	1.273023286502782E-007
Bounce:Time:	2393.5889691107	Magnetic Field Strength:	1.275031820880119E-007
Bounce:Time:	2485.89049457933	Magnetic Field Strength:	1.276672836686169E-007
Bounce:Time:	2578.43069224157	Magnetic Field Strength:	1.278018551687122E-007
Bounce:Time:	2671.18448989841	Magnetic Field Strength:	1.278270734281715E-007
Bounce:Time:	2764.14148755012	Magnetic Field Strength:	1.278822895843127E-007
Bounce:Time:	2857.26968519751	Magnetic Field Strength:	1.279272476714980E-007
Bounce:Time:	2950.56528284066	Magnetic Field Strength:	1.279657301253406E-007
Bounce:Time:	3044.00468048018	Magnetic Field Strength:	1.280002714139339E-007
Bounce:Time:	3137.57927811629	Magnetic Field Strength:	1.279853761629201E-007
Bounce:Time:	3231.27627574930	Magnetic Field Strength:	1.280258225145481E-007

Bounce:Time:	3325.09467337925	Magnetic Field Strength:	1.280657154545046E-007
Bounce:Time:	3419.02607100634	Magnetic Field Strength:	1.281051851806443E-007
Bounce:Time:	3513.05706863092	Magnetic Field Strength:	1.280825018009166E-007
Bounce:Time:	3607.17546625329	Magnetic Field Strength:	1.281143187782469E-007
Bounce:Time:	3701.36366387390	Magnetic Field Strength:	1.281809884273960E-007
Bounce:Time:	3795.62226149272	Magnetic Field Strength:	1.282166078785924E-007
Bounce:Time:	3889.93285911024	Magnetic Field Strength:	1.282454290175728E-007
Bounce:Time:	3984.27765672689	Magnetic Field Strength:	1.282245162264074E-007
Bounce:Time:	4078.65045434283	Magnetic Field Strength:	1.282456246931002E-007
Bounce:Time:	4173.03785195840	Magnetic Field Strength:	1.282743174812925E-007
Bounce:Time:	4267.43604957371	Magnetic Field Strength:	1.283447314959480E-007
Bounce:Time:	4361.82404718926	Magnetic Field Strength:	1.283653490486837E-007
Bounce:Time:	4456.19384480528	Magnetic Field Strength:	1.283793262189630E-007
Bounce:Time:	4550.53024242214	Magnetic Field Strength:	1.283622026351576E-007
Bounce:Time:	4644.82084004016	Magnetic Field Strength:	1.283800479855395E-007
Bounce:Time:	4739.05623765958	Magnetic Field Strength:	1.284512424413172E-007
Bounce:Time:	4833.22503528067	Magnetic Field Strength:	1.284603056982973E-007
Bounce:Time:	4927.30883290392	Magnetic Field Strength:	1.284692579285167E-007
Bounce:Time:	5021.30963052926	Magnetic Field Strength:	1.284779997123066E-007
Bounce:Time:	5115.21422815703	Magnetic Field Strength:	1.285422733690516E-007
Bounce:Time:	5209.01222578749	Magnetic Field Strength:	1.285547891338780E-007
Bounce:Time:	5302.70002342074	Magnetic Field Strength:	1.285634957753797E-007
Bounce:Time:	5396.24942105748	Magnetic Field Strength:	1.285651336708781E-007
Bounce:Time:	5489.65681869781	Magnetic Field Strength:	1.285555018519469E-007
Bounce:Time:	5582.88741634261	Magnetic Field Strength:	1.285701653435561E-007
Bounce:Time:	5675.92901399218	Magnetic Field Strength:	1.284737612932229E-007
Bounce:Time:	5768.76421164697	Magnetic Field Strength:	1.283480345335540E-007
Bounce:Time:	5861.39720930686	Magnetic Field Strength:	1.281878949939904E-007
Bounce:Time:	5953.82000697206	Magnetic Field Strength:	1.280791150970443E-007
Bounce:Time:	6046.05420464203	Magnetic Field Strength:	1.279109997336853E-007
Bounce:Time:	6138.10160231672	Magnetic Field Strength:	1.277454210509561E-007
Bounce:Time:	6229.98339999559	Magnetic Field Strength:	1.275909540406048E-007
Bounce:Time:	6321.70679767846	Magnetic Field Strength:	1.274963954752747E-007
Bounce:Time:	6413.28379536503	Magnetic Field Strength:	1.273459785563059E-007
Bounce:Time:	6504.72679305499	Magnetic Field Strength:	1.271994601361561E-007
Bounce:Time:	6596.04599074807	Magnetic Field Strength:	1.271049893777513E-007
Bounce:Time:	6687.25658844390	Magnetic Field Strength:	1.270234207278559E-007
Bounce:Time:	6778.37398614208	Magnetic Field Strength:	1.268925312284659E-007
Bounce:Time:	6869.41018384231	Magnetic Field Strength:	1.267635662960939E-007
Bounce:Time:	6960.37898154424	Magnetic Field Strength:	1.266448916328006E-007
Bounce:Time:	7051.29317924756	Magnetic Field Strength:	1.265669164855062E-007
Bounce:Time:	7142.16457695195	Magnetic Field Strength:	1.264524782359043E-007
Bounce:Time:	7233.00297465718	Magnetic Field Strength:	1.263410159009808E-007
Bounce:Time:	7323.83037236269	Magnetic Field Strength:	1.262691933002271E-007
Bounce:Time:	7414.65697006822	Magnetic Field Strength:	1.261697822411873E-007
Bounce:Time:	7505.49196777353	Magnetic Field Strength:	1.260758240579629E-007
Bounce:Time:	7596.35176547822	Magnetic Field Strength:	1.259860693510645E-007
Bounce:Time:	7687.24276318212	Magnetic Field Strength:	1.259131188941304E-007
Bounce:Time:	7778.18056088484	Magnetic Field Strength:	1.258053198820528E-007
Bounce:Time:	7869.19175858570	Magnetic Field Strength:	1.257493933089352E-007
Bounce:Time:	7960.29215628431	Magnetic Field Strength:	1.257375134040385E-007
Bounce:Time:	8051.46435398111	Magnetic Field Strength:	1.257694834797609E-007
Bounce:Time:	8142.65215167751	Magnetic Field Strength:	1.258764080801012E-007
Bounce:Time:	8233.77554937554	Magnetic Field Strength:	1.260021331556987E-007
Bounce:Time:	8324.84434707495	Magnetic Field Strength:	1.260848284191374E-007
Bounce:Time:	8415.85734477577	Magnetic Field Strength:	1.262065505229655E-007
Bounce:Time:	8506.82634247770	Magnetic Field Strength:	1.263281499646473E-007

Bounce:Time:	8597.76294018044	Magnetic Field Strength:	1.264504542541695E-007
Bounce:Time:	8688.68193788364	Magnetic Field Strength:	1.265704963995139E-007
Bounce:Time:	8779.59613558695	Magnetic Field Strength:	1.267107663717330E-007
Bounce:Time:	8870.51593329012	Magnetic Field Strength:	1.268562092406905E-007
Bounce:Time:	8961.45593099279	Magnetic Field Strength:	1.270058459035541E-007
Bounce:Time:	9052.42932869460	Magnetic Field Strength:	1.271301045218337E-007
Bounce:Time:	9143.44952639524	Magnetic Field Strength:	1.272927988927181E-007
Bounce:Time:	9234.52692409443	Magnetic Field Strength:	1.274597132741842E-007
Bounce:Time:	9325.67352179188	Magnetic Field Strength:	1.275908653486421E-007
Bounce:Time:	9416.90511948717	Magnetic Field Strength:	1.277614365514399E-007
Bounce:Time:	9508.23471717999	Magnetic Field Strength:	1.279434846803180E-007
Bounce:Time:	9599.68231486983	Magnetic Field Strength:	1.281287621850766E-007
Bounce:Time:	9691.25691255646	Magnetic Field Strength:	1.282213605145253E-007
Bounce:Time:	9782.96971023960	Magnetic Field Strength:	1.284144564713573E-007

Trial run #3:

Mass: 1.672621580000000E-027 Charge: 1.602176460000000E-019
Energy: 100000.000000000 Pitch Angle: 45.0000000000000
Initial Position: 0.0000000000000 15.0000000000000 0.0000000000000
Bo: 1.036958604384613E-008 Vo: 4376947.36843198
Bounce Time: 79.0404416369476 Btp: 2.073917118115426E-008
Average drift period: 2179.35259698827

Bounce:Time:	20.3674343749444	Magnetic Field Strength:	2.000336132653095E-008
Bounce:Time:	59.6900333815720	Magnetic Field Strength:	2.005690561451668E-008
Bounce:Time:	99.0758323866030	Magnetic Field Strength:	2.008488691768141E-008
Bounce:Time:	138.671031386344	Magnetic Field Strength:	2.008513101004919E-008
Bounce:Time:	178.584230378052	Magnetic Field Strength:	2.004740660136807E-008
Bounce:Time:	218.777829362676	Magnetic Field Strength:	1.999168827561370E-008
Bounce:Time:	259.124628343430	Magnetic Field Strength:	1.996697151058286E-008
Bounce:Time:	299.510627323194	Magnetic Field Strength:	1.997493903830852E-008
Bounce:Time:	339.811426305110	Magnetic Field Strength:	2.001567416899659E-008
Bounce:Time:	379.917225291952	Magnetic Field Strength:	2.008176031873101E-008
Bounce:Time:	419.706824286783	Magnetic Field Strength:	2.009763151082367E-008
Bounce:Time:	459.214423288737	Magnetic Field Strength:	2.008634469677415E-008
Bounce:Time:	498.582222294222	Magnetic Field Strength:	2.004476805199295E-008
Bounce:Time:	537.953221299627	Magnetic Field Strength:	1.998692755982853E-008
Bounce:Time:	577.336420304724	Magnetic Field Strength:	2.004319061046302E-008
Bounce:Time:	616.704219310210	Magnetic Field Strength:	2.008903746086102E-008
Bounce:Time:	656.196818312543	Magnetic Field Strength:	2.010532748918449E-008
Bounce:Time:	695.958217308085	Magnetic Field Strength:	2.009419441733742E-008
Bounce:Time:	736.045416295397	Magnetic Field Strength:	2.003105670915635E-008
Bounce:Time:	776.351415277182	Magnetic Field Strength:	1.998809434355323E-008
Bounce:Time:	816.764614256259	Magnetic Field Strength:	1.997749086520341E-008
Bounce:Time:	857.161213235755	Magnetic Field Strength:	1.999968308608325E-008
Bounce:Time:	897.421412218697	Magnetic Field Strength:	2.005260044311360E-008
Bounce:Time:	937.424011208146	Magnetic Field Strength:	2.010292947389902E-008
Bounce:Time:	977.108010205644	Magnetic Field Strength:	2.010538816920049E-008
Bounce:Time:	1016.57200920870	Magnetic Field Strength:	2.008202384960375E-008
Bounce:Time:	1055.95960821368	Magnetic Field Strength:	2.002959279727429E-008
Bounce:Time:	1095.38760721765	Magnetic Field Strength:	2.004041983638034E-008
Bounce:Time:	1134.76100622299	Magnetic Field Strength:	2.009654456732872E-008
Bounce:Time:	1174.17920522721	Magnetic Field Strength:	2.012808120113564E-008
Bounce:Time:	1213.78960422656	Magnetic Field Strength:	2.013325331824194E-008
Bounce:Time:	1253.71800321789	Magnetic Field Strength:	2.010580405498597E-008
Bounce:Time:	1293.93960220180	Magnetic Field Strength:	2.004686143794314E-008
Bounce:Time:	1334.32660118154	Magnetic Field Strength:	2.001767779598901E-008
Bounce:Time:	1374.76520015998	Magnetic Field Strength:	2.002244075552309E-008

Bounce:Time:	1415.13219914022	Magnetic Field Strength:	2.005792326264194E-008
Bounce:Time:	1455.31679812507	Magnetic Field Strength:	2.012333585979504E-008
Bounce:Time:	1495.19219711774	Magnetic Field Strength:	2.014155992065629E-008
Bounce:Time:	1534.76899611794	Magnetic Field Strength:	2.013391069068933E-008
Bounce:Time:	1574.19139512205	Magnetic Field Strength:	2.009459005572338E-008
Bounce:Time:	1613.60359412641	Magnetic Field Strength:	2.003454338851660E-008
Bounce:Time:	1653.07919312918	Magnetic Field Strength:	2.004684205374994E-008
Bounce:Time:	1692.53359213247	Magnetic Field Strength:	2.009620148550556E-008
Bounce:Time:	1732.09899113297	Magnetic Field Strength:	2.011438980075508E-008
Bounce:Time:	1771.92159012696	Magnetic Field Strength:	2.010785434340118E-008
Bounce:Time:	1812.07258911266	Magnetic Field Strength:	2.004607508935114E-008
Bounce:Time:	1852.45798809244	Magnetic Field Strength:	2.000115483207377E-008
Bounce:Time:	1892.95718706935	Magnetic Field Strength:	1.998578905701505E-008
Bounce:Time:	1933.44958604642	Magnetic Field Strength:	2.000824845842127E-008
Bounce:Time:	1973.81438502672	Magnetic Field Strength:	2.005918658212768E-008
Bounce:Time:	2013.92818401336	Magnetic Field Strength:	2.011387582261369E-008
Bounce:Time:	2053.72098300811	Magnetic Field Strength:	2.011727303659790E-008
Bounce:Time:	2093.28238200871	Magnetic Field Strength:	2.009480342048919E-008
Bounce:Time:	2132.76038101141	Magnetic Field Strength:	2.004342694464063E-008
Bounce:Time:	2172.28078001304	Magnetic Field Strength:	2.000936388856628E-008
Bounce:Time:	2211.77197901541	Magnetic Field Strength:	2.006897167699244E-008
Bounce:Time:	2251.30197801680	Magnetic Field Strength:	2.010208555290968E-008
Bounce:Time:	2291.01857701347	Magnetic Field Strength:	2.010911202961067E-008
Bounce:Time:	2331.05017600219	Magnetic Field Strength:	2.008543194293609E-008
Bounce:Time:	2371.38237498331	Magnetic Field Strength:	2.002587129906940E-008

Shown here is the data for the simulation of three 1 MeV protons starting at initial positions 4 Re apart in the radial direction. The format of the data is particle number, time, energy(EV), parallel velocity, magnitude of perpendicular velocity. Notice that the energy is fluctuating as the result of the work done by the electric field.

1	0.000	100000.000	9787151.636	9787152.064
1	10.000	1002765.437	11480390.683	7765764.972
1	20.002	999269.304	6297793.760	12319679.062
1	30.002	999982.055	-7814939.026	11423658.468
1	40.003	1002918.907	-11697060.199	7437382.592
1	50.003	999227.386	-4151071.524	13198381.455
1	60.004	1001848.419	10626056.560	8889191.108
1	70.004	1001780.211	10595676.122	8924649.965
1	80.004	1000377.763	-2488367.628	13618262.731
1	90.005	1002015.277	-11291481.911	8029022.300
1	100.005	1001816.460	-10890337.601	8563014.715
1	110.007	1002014.899	-650742.975	13839769.645
1	120.008	1001859.425	10564927.007	8961876.059
1	130.009	1001501.508	11378662.103	7898758.465
1	140.011	1003767.823	529925.252	13857044.741

1	150.012	1001178.613	-11548257.080	7644621.363
1	160.012	1003308.585	-7866680.755	11416035.403
1	170.013	1002346.509	10034065.221	9557392.647
1	180.014	1001606.883	10878979.888	8575098.865
1	190.014	1005139.762	-3761602.336	13357083.857
1	200.014	1000494.538	-11768166.196	7292577.665
1	210.016	1002959.629	-9322777.105	10258143.382
1	220.016	1004425.969	6501826.705	12253605.373
1	230.016	1000235.597	11914847.554	7046859.246
1	240.017	1004032.057	7157627.572	11879288.626
1	250.018	1002217.618	-10094138.254	9492623.420
1	260.019	1001680.575	-10729049.027	8762770.599
1	270.020	1003257.165	7573753.477	11612016.955
1	280.022	1000997.663	11608824.340	7550033.717
1	290.022	1003375.836	-2683935.548	13602202.179
1	300.023	1001076.392	-11909436.634	7067404.988
1	310.023	1001895.316	-8450572.776	10978506.313
1	320.024	1001514.013	8296304.315	11092252.564
1	330.025	1001696.322	11969624.170	6973503.820
1	340.025	1000525.205	4299218.137	13160320.023
1	350.027	1001532.641	-11047964.103	8355404.848
1	360.027	1001056.191	-10043330.559	9534701.648
1	370.028	1000436.503	9231293.003	10317147.669
1	380.030	1001669.111	11078789.555	8316060.805
1	390.031	999186.324	-7311327.975	11745862.442
1	400.032	1002670.965	-11880038.905	7138140.719
1	410.034	997394.473	-630899.622	13808674.450
1	420.035	1002421.741	11680357.731	7457202.898
1	430.035	1000609.108	10008563.104	9566715.118
1	440.036	999080.366	-7502343.095	11623912.869
1	450.036	1003005.565	-12070121.900	6816497.357
1	460.038	997602.693	-711751.019	13806187.923
1	470.039	1002936.884	12128992.228	6710206.299
1	480.040	998416.135	2242281.374	13647176.458
1	490.041	1002709.194	-12155741.756	6658351.406
1	500.042	999528.859	-2399145.189	13628298.698
1	510.043	1002258.873	12044482.940	6851267.092
1	520.044	1001121.779	7306335.698	11764737.484
1	530.044	1001812.039	-10922912.478	8521373.718
1	540.045	1001794.101	-10873305.670	8584382.003
1	550.047	1002519.019	7614125.639	11579480.071
1	560.047	1001370.279	11979147.019	6952642.154
1	570.048	1003868.944	-5179684.490	12864243.105
1	580.049	1001151.902	-11907938.380	7070952.107
1	590.049	1003889.448	8034822.796	11303248.770
1	600.000	1001957.132	11058218.049	8346702.163
2	0.000	1000000.000	9787151.636	9787152.064
2	10.000	999593.251	-8384278.268	11009206.914
2	20.001	998768.958	4649240.326	13027870.437
2	30.001	998541.317	-312132.938	13827501.803
2	40.002	998995.957	-3779771.726	13307804.371
2	50.002	999601.305	7245664.300	11789853.728
2	60.002	999992.467	-9724329.516	9849500.237
2	70.002	999985.768	10792839.287	8665366.487
2	80.003	999861.733	-10635251.319	8856727.575
2	90.004	1000022.099	9411129.439	10149461.023
2	100.005	1000487.003	-7460211.026	11662556.863

2	110.006	1001060.115	4826551.707	12980145.403
2	120.007	1001627.142	-1194013.582	13800823.769
2	130.007	1001502.231	-3541573.198	13391106.541
2	140.008	1000687.693	7607607.678	11568609.855
2	150.009	999789.915	-9864125.143	9707495.583
2	160.009	999296.747	10782195.817	8670998.165
2	170.010	999303.925	-10881710.355	8545859.266
2	180.010	999565.170	10514028.481	8997143.126
2	190.010	999899.172	-9606575.511	9963487.008
2	200.012	1000133.596	7544083.342	11605562.589
2	210.013	1000051.963	-3467998.256	13399986.035
2	220.014	999704.762	-1818861.527	13719032.934
2	230.015	999600.085	6338842.290	12301184.770
2	240.016	999807.067	-8822815.752	10662909.702
2	250.017	1000172.823	10084274.182	9482468.338
2	260.017	1000553.371	-10761388.281	8710638.206
2	270.017	1000714.213	10940762.325	8486060.867
2	280.018	1000342.157	-10283864.022	9267382.193
2	290.019	999525.237	8446989.114	10960570.426
2	300.020	998704.799	-5056622.586	12874747.394
2	310.021	998344.694	1040354.412	13790475.965
2	320.022	998654.212	2406190.700	13620906.996
2	330.023	999225.843	-5369287.030	12751436.355
2	340.023	999738.606	8034158.367	11268491.695
2	350.025	1000008.546	-9979409.320	9591126.601
2	360.026	999944.969	10875731.204	8560643.133
2	370.028	999784.836	-10966342.210	8442440.453
2	380.029	999797.177	10463866.692	9057887.194
2	390.029	1000022.112	-9676633.701	9896649.891
2	400.030	1000430.183	8529462.554	10904465.338
2	410.030	1001035.896	-6518119.054	12218398.428
2	420.031	1001729.969	2923095.508	13541182.261
2	430.031	1001869.951	1586621.115	13762905.039
2	440.031	1001228.595	-5701273.473	12621708.824
2	450.032	1000535.598	8223164.682	11138171.010
2	460.033	1000041.050	-9530540.604	10037596.456
2	470.034	999761.327	10326666.903	9213626.277
2	480.035	999677.204	-10864955.060	8571323.932
2	490.035	999787.451	11047852.392	8335521.629
2	500.036	999940.703	-10584938.087	8917645.904
2	510.037	999860.881	9258677.106	10287221.634
2	520.038	999460.732	-7093479.201	11880905.873
2	530.039	998940.735	4674359.774	13020142.585
2	540.039	998413.200	-1974232.209	13688502.328
2	550.040	998189.649	-1413935.441	13756113.118
2	560.040	998642.408	5396544.162	12735537.321
2	570.041	999440.863	-8483164.763	10931856.232
2	580.041	1000209.651	10178286.491	9381861.809
2	590.042	1000622.661	-10923520.431	8507212.907
2	600.000	1000669.925	11117594.420	8252521.973
3	0.000	1000000.000	9787151.636	9787152.064
3	10.001	1000135.980	-10200881.758	9356534.861
3	20.001	999559.184	8360818.960	11026737.453
3	30.002	999069.360	-3470611.255	13392283.273
3	40.002	999371.217	-3173625.724	13467899.696
3	50.003	999724.874	7883738.464	11374121.623
3	60.004	999623.547	-10010065.408	9555268.365

3	70.006	999436.281	10242159.248	9304131.402
3	80.006	999786.591	-8246736.111	11114276.491
3	90.006	1000591.627	3155028.073	13480942.937
3	100.007	1000660.316	3337368.601	13437453.427
3	110.008	999905.930	-8029449.313	11273269.483
3	120.009	999292.833	10108735.417	9447469.200
3	130.009	999370.741	-10134325.785	9420805.282
3	140.010	999898.850	7668355.754	11521875.921
3	150.011	999991.742	-2446233.608	13623180.309
3	160.011	999621.595	-3871006.782	13286063.958
3	170.012	999585.804	8241543.508	11116397.481
3	180.013	999950.470	-10209865.987	9344829.070
3	190.013	1000007.326	10012560.346	9556501.527
3	200.014	999375.240	-7536125.115	11604473.772
3	210.015	998644.978	2666095.380	13572362.631
3	220.015	998758.772	3599403.339	13356016.916
3	230.015	999549.380	-8230830.980	11124017.967
3	240.015	1000036.416	10283221.261	9264934.954
3	250.017	999833.022	-9966365.433	9602929.425
3	260.018	999581.696	7501143.103	11628817.545
3	270.018	999806.592	-2334326.258	13641501.059
3	280.019	1000098.909	-4175979.389	13196849.150
3	290.020	999737.817	8819076.523	10665380.625
3	300.021	999226.012	-10408409.589	9115558.924
3	310.022	999436.436	9680416.405	9887277.436
3	320.023	1000218.544	-6651507.505	12139851.664
3	330.023	1000800.107	734701.523	13827153.652
3	340.025	1000212.108	5895933.189	12524188.172
3	350.026	999513.553	-9637443.556	9929913.017
3	360.027	999493.537	10414054.810	9111921.781
3	370.028	999713.813	-9160749.396	10373163.763
3	380.029	999558.563	5426784.483	12729576.736
3	390.029	999078.828	1062179.656	13793911.050
3	400.030	999328.711	-7232326.835	11795826.718
3	410.030	1000010.039	10033750.441	9534278.052
3	420.031	1000173.959	-10358621.979	9181991.056
3	430.032	999622.481	8771313.000	10703664.194
3	440.032	998871.272	-4519266.220	13074275.413
3	450.032	998865.131	-2547126.409	13596742.820
3	460.033	999605.854	8129597.877	11198696.885
3	470.033	999824.197	-10270651.069	9276676.646
3	480.033	999657.382	10223052.088	9327392.512
3	490.033	999727.049	-8023966.815	11275652.889
3	500.034	1000325.930	2438046.439	13626997.203
3	510.035	1000364.710	5058072.447	12886522.253
3	520.036	999599.205	-9322504.732	10226964.614
3	530.036	999133.314	10505750.002	9002214.326
3	540.038	999495.886	-9598077.557	9967798.823
3	550.038	1000298.808	5944558.174	12501846.080
3	560.039	1000490.361	1285129.196	13784740.379
3	570.040	999803.400	-7543224.283	11603395.453
3	580.041	999594.885	10125296.021	9432786.040
3	590.042	999759.048	-10390514.902	9141538.272
3	600.001	999650.742	8414108.468	10986926.394

Acknowledgment

Special thanks to Dr. John Guillory from George Mason University, the author's mentor who gave much support and guidance.

Bibliography

- [1] Birdsall, C. K., and Langdon, A. B. Plasma Physics via Computer Simulation. IOP Publishing Ltd, 1991.
- [2] Book, David L. NRL Plasma Formulary. Naval Research Laboratory, 1980.
- [3] Gaffey, John D. Jr., Bilitza, Dieter. “NASA/National Space Science Data Center Trapped Radiation Models.” Journal of Spacecraft and Rockets 31.2 (1994): 172-176.
- [4] Golant, V., Zhilinsky, and Sakharov, A. Fundamentals of Plasma Physics. Wiley, 1980.
- [5] Green, James L. The Magnetosphere.
<http://ssdoo.gsfc.nasa.gov/education/lectures/magnetosphere/index.html>
- [6] Krall, N. A., and Trivelpiece, A. W. Principles of Plasma Physics. San Francisco Press, 1986.
- [7] Lyon, John G. “Numerical methods used in the Lyon-Fedder-Mobarry Global code to model the magnetosphere.” Proceedings of ISSS-7, 26-31 March, 2005.
- [8] Parks, G. K. Physics of Space Plasmas. Addison Wesley, 1991.
- [9] Press, William H. Numerical Recipes in Fortran 90. Cambridge University Press, 1996.
- [10] Shene, C. K. Fortran 90 Tutorial. 20 Aug. 1998
<http://www.cs.mtu.edu/shene/COURSES/cs201/NOTES/fortran.html>

- [11] Wentworth, R. C. “Pitch Angle Diffusion in a Magnetic Mirror Geometry.” The Physics of Fluids 6.2 (1963): 431-437.
- [12] Wright, Richard S. Jr., and Lipchak, Benjamin. OpenGL Superbible. Sams Publishing, 2005.